



Recent and future changes in rain-on-snow event characteristics across Svalbard

Hannah Vickers¹, Priscilla Mooney¹ and Oskar Landgren²

¹NORCE Norwegian Research Centre, Bergen, Norway

²Norwegian Meteorological Institute, Oslo, Norway

Correspondence to: Hannah Vickers (havi@norce-research.no)

Abstract.

Rain-on-snow (ROS) events in Svalbard are becoming a more frequent occurrence during the winter season due to rapid and ongoing climate warming across the Arctic. ROS events have gained increasing attention in recent decades due to their cascading impacts on the physical environment, and terrestrial and marine ecosystems that are impacted by snowmelt. While the frequency of ROS events in Svalbard has been well studied and documented, other characteristics of ROS, such as their duration, intensity and seasonal timing have received less attention. Such characteristics are equally important to quantify due to their potential consequences for the winter snowpack and snow-dependent ecosystems. This study addresses this knowledge gap using the Copernicus Arctic Regional Reanalysis (CARRA) for the present-day analysis and km-scale climate projections from a regional climate model for the future period of 2030-2070 under the high emissions scenario SSP5-8.5. For the present climate, the results show significant and increasing trends in all characteristics but confined mainly to low-lying areas of Nordaustlandet and some areas in the east of the archipelago, while no statistically significant trend was found in the southern and western areas which typically exhibit the largest values in all characteristics. Analysis of the future projections showed that the largest changes relative to present day conditions in all ROS characteristics will take place over the mountainous and glaciated areas in the north and northeast of the archipelago, while some low lying western coastal areas will experience a decrease. This reduction is expected to be the result of fewer days with snow, shortening the season where rain can fall on an existing snow cover. Moreover, while ROS has increased most in November and February, the future climate simulation features a substantial increase in ROS events in April, which experiences very few, if any, ROS events in the present climate, which may lead to considerable changes in snow hydrology. Further work could include analysing an ensemble of climate projections for Svalbard to produce a range of ROS scenarios, as well as carrying out a more in-depth analysis of the hydrological impacts associated with the changes in ROS characteristics identified here.



1 Introduction

The Arctic is warming at a rate that is three to four times the global average (Rantanen et al., 2022) resulting in substantial changes to the wintertime climate. Interludes of winter warming bringing rain, often referred to as rain-on-snow (ROS) events, are becoming increasingly frequent across the High Arctic Archipelago of Svalbard. These events have attracted increasing research attention during the most recent decade and as such their spatiotemporal characteristics, meteorological drivers and impacts are becoming better understood and documented using a wide range of observational approaches (e.g. Bartsch et al., 2023; Vickers et al., 2022; Serreze et al., 2021; Wickström et al., 2020; Peeters et al., 2019; Forbes et al., 2016). These studies include not only their impacts on the cryosphere, but also on terrestrial and marine/coastal ecosystems as well as society. A significant consequence of ROS events is the formation of ground ice as rain percolates through the snowpack to the ground-snow interface and refreezes. This presents a significant barrier to winter forage for reindeer populations in Finnmark and Svalbard and has in some extreme cases resulted in starvation and large die-offs (e.g., Hansen et al., 2014) as well as adaptations to foraging habits (Pedersen et al., 2021). The impact of ROS events on the snowpack is largely dependent on the characteristics of a ROS event, such as the total precipitation and duration, and thus the intensity - as well as the initial properties of the snowpack itself. Snow depth and snowpack stratigraphy is an important factor which determines how rain percolates through the snowpack and consequently, if ground ice forms following a ROS event (Peeters et al., 2019) and how surface runoff and hydrology is affected (eg., Würzer et al., 2016). Indeed, if a ROS event is intense enough, and the snowpack is thin enough, complete ablation of the snow cover may occur, removing the wintertime insulation of permafrost as well as increasing the availability of forage to reindeer. Therefore, the timing and seasonality of ROS events is also an important factor, as this dictates the initial thickness of the snowpack being impacted.

To understand which areas are most vulnerable to ROS impacts at present and in the future, reliable datasets describing the spatial and temporal variations in ROS are crucial. Recent studies of ROS climatology in Svalbard have exploited Synthetic Aperture Radar (SAR) remote sensing, due to its sensitivity to liquid water in the snowpack (Vickers et al., 2022). This dataset was compared to ROS events detected using snow models and atmospheric reanalysis, and good agreement with the SAR dataset was obtained once the models and reanalysis datasets had been calibrated against ground observations recorded at three sites across Spitsbergen (Ny Ålesund, Longyearbyen and Hornsund). However, it was shown that different temperature thresholds were required to produce the best accuracy of ROS detection with respect to the ground observations (Vickers et al., 2024). Specifically, it was found that gridded atmospheric reanalyses provided by the Copernicus Arctic Regional Reanalysis (CARRA) dataset was able to capture the frequency of ROS events very accurately when evaluated against ground observations. Until now most ROS studies of Svalbard have concentrated on documenting ROS frequency, but little attention has been paid to their duration, intensity, and timing. Earlier analyses of downscaled global climate model (GCM) simulations have highlighted a potential threefold increase in mild weather days during the winter (October-April) season by 2100, where precipitation falls on days with temperature above freezing point (Isaksen et al., 2017) while others note an increase exceeding 20% in winter rainfall projected at Longyearbyen airport (Førland et al., 2011) with greatest changes expected in the north and



northeast of the archipelago. As climate warming continues to change the wintertime climate in Svalbard, it is crucial to quantify how ROS characteristics are influenced by changes in climate, as changes in ROS characteristics will also to a large degree determine the severity of their impact on snowpack stratigraphy and properties, and therefore their impacts on ecosystems. Moreover, it is of equal importance to advance our understanding of how these characteristics are likely to change in the coming decades, such that measures can be planned that will minimise the impacts of ROS on nature and society. Determining possible future changes to ROS climatology across Svalbard has become feasible due to recent advances in climate modelling and high-performance computing that allow climate models to run at convection-permitting (hereafter, km) scales. These scales are important for Svalbard as its climate has a large spatial variability arising from its complex topography, coastlines, fjords, glaciers and surrounding sea ice (Hanssen-Bauer et al. 2019). The benefits of such km-scale climate projections have been demonstrated already by numerous studies (Mooney et al. 2020; Køltzow et al. 2019; Prein et al. 2015). Rain-on-snow studies benefit further from these scales as climate models at these resolutions better resolve convective processes and the separation of precipitation into rain and snow is physically based as opposed to the temperature-based approaches used in coarser resolution models (Mooney and Li, 2021). Specifically for Svalbard, Landgren et al. (2025) produced 2.5 km simulations using the HCLIM-AROME regional climate model with input from the global Earth System Model MPI-ESM1-2-LR under the future scenario SSP5-8.5 (from now on HCLIM-MPI). The fine resolution allows a much-improved representation of the valleys and mountains on Svalbard. The CARRA dataset now spans more than 30 years, providing an ideal opportunity to exploit the full time series to document changes in the characteristics of ROS since 1991. We have derived parameters that include their timing/seasonality, duration, total precipitation, and intensity, as well as frequency. In addition to studying the spatial variations in these parameters, we also quantify trends in these characteristics over climate-relevant timescales (1991-2023). Lastly, we use high resolution climate projections from the HCLIM-MPI dataset to firstly estimate how well these specific characteristics are represented in the present climate, by comparing the results to those obtained with CARRA and how they can be expected to change under an SSP5-8.5 warming scenario in the next four decades until 2070.

2 Methods and Datasets

2.1 Study area

The Svalbard archipelago is located in the North Atlantic Ocean, spanning latitudes between 74 and 81°N and comprises five main islands, with Spitsbergen being the largest island (Fig.1). Wintertime sea ice is found just north and north-east of Svalbard, while to the west of the archipelago is the West Spitsbergen Current. The climate of Svalbard is therefore heavily affected by the location of the sea ice edge, contributing to a strong a southwest-northeast gradient, with milder coastal climates in the west and south, and cold inland climate influenced by sea ice presence and variability in the north and east (Day et al., 2012). Annual precipitation at Longyearbyen airport, in the central part of Svalbard ranges from 121.8mm (2021) to 310mm (2016), while Ny Ålesund in the northwest part of Svalbard, experiences a substantially wetter climate with annual precipitation



ranging from 205mm (2019) to 749mm (2018). The occurrence of wintertime ROS events is reflected by the climatic gradient, with highest frequency in the south and west and very few events per winter in the north and east (e.g., Wickström et al., 2020; Vickers et al., 2022, 2024).



Figure 1: Overview of the Svalbard archipelago, showing the main islands (Spitsbergen, Nordaustlandet, Edgeøya, Barentsøya). Bjørnøya lies farthest south and is not shown (source: <https://toposvalbard.npolar.no/> courtesy of the Norwegian Polar Institute).

2.2 CARRA dataset

In this study we use data from the East domain of the Copernicus Arctic Regional Reanalysis (CARRA) dataset, which covers all of Svalbard and its surrounding waters. CARRA provides 3-hourly reanalyses and short-term hourly forecasts of atmospheric and surface meteorological variables at 2.5 km resolution (Schyberg et al., 2020). Earlier evaluations of CARRA have already demonstrated its added value compared to other reanalysis datasets for Svalbard (Køltzow et al., 2022). Following the approach outlined by Vickers et al. (2024), we use the 2m air temperature and snow water equivalent (SWE) reanalyses at 3-hourly resolution and averaged the data to daily values. Forecasted precipitation data at lead times of +6 and +30 hours with initial time 00UT were obtained and the difference was used to calculate the 24-hour accumulated precipitation values from 0600 UTC to 0600 UTC the following day. CARRA data were obtained from 1991 to 2023 to analyse trends for the present-day climate, while only a part of the dataset overlapping with the historical period of the HCLIM simulations was used for



model evaluation (2000-2020). Based on the calibration approach described in the earlier study by Vickers et al., 2024, a rain-on-snow *day* was detected when the daily mean 2m temperature was $>-0.5^{\circ}\text{C}$, daily precipitation was $>1\text{mm}$ and SWE was $>2\text{mm}$, since these thresholds produced the highest accuracy of ROS day detection when evaluated against in-situ observations.

2.3 HCLIM km-scale climate model data

This dataset consists of km-scale climate simulations of Svalbard covering the period 1991-2070 and is detailed in Landgren et al. (2025). The data was produced by dynamically downscaling the Max Planck Institute for Meteorology Earth System Model Version 1.2 at Low Resolution (MPI-ESM1-2-LR, Gutjahr et al., 2019) under SSP5-8.5 with the HARMONIE Climate (HCLIM, Belušić et al. 2020, Wang 2024) cycle 43 regional climate model to 2.5 km horizontal grid spacing. For evaluation of present climate conditions, the dataset also consists of a dynamical downscaling of the 5th generation ECMWF Reanalysis (ERA5, Hersbach et al. 2020) with HCLIM for the same domain and resolution but only covering the period 2000-2020. The HCLIM model features convection-permitting HARMONIE-AROME atmospheric physics and SURFEX land-surface model with ISBA Explicit Snow scheme. More details and evaluation of the simulations are available in Landgren et al. (2025). From hereon the HCLIM simulations produced by downscaling the ERA5 Reanalysis data will be referred to as HCLIM-ERA5 and the data produced by downscaling MPI-ESM1-2-LR will be referred to as HCLIM-MPI for clarity.

To identify ROS days in the HCLIM-ERA5 simulations for comparison with the CARRA results for the present climate (2000-2020), we applied the same thresholds as was used for the CARRA dataset, to the variables *pr*, *tas* and *snd*, where *pr* is the accumulated precipitation, which includes both solid and liquid precipitation, *tas* is the 2m air temperature and *snd* is the snow depth water equivalent. All variables are available at 3-hourly intervals, but for the purpose of producing comparable results to CARRA, we have produced daily mean values for the 2m air temperature and snow depth water equivalent variables, and a total daily precipitation estimate by taking the difference between the maximum values of the accumulated precipitation for the following day and the current day. In addition, a *prrain* (accumulated rain) variable was also made available from the RCM simulation to assess the impacts of different approaches for separating rain and snow on the results. The *prrain* variable is derived from the microphysical scheme of the RCM and uses a physics-based approach to separate snow and rain. This contrasts with the approach used in this study which separates rain from snow in the precipitation variables using a temperature threshold-based approach. To detect ROS using *prrain*, we applied the same daily precipitation threshold as we used for the CARRA total daily precipitation (1 mm) and to the snow depth water equivalent (2 mm). We have included the analysis of the ROS characteristics in the present and future climate using the *prrain* variable in the Appendix (Fig.A2 to A4).

2.4 Definition of ROS event characteristics

For the purposes of this study, a rain-on-snow event is defined as consecutive rain-on-snow days where the criteria for detection were met. By using this definition, a rain-on-snow *event* can be characterised by its duration, which in turn determines the total precipitation as rain that fell during the event and thereby the average intensity of the event, given by the total precipitation



divided by the duration. ROS events are detected in the period 1 November to 30 April, and *for each winter season* the ROS events with longest duration, greatest total precipitation and highest intensity are identified, as well as the mean values of ROS duration, total precipitation, and intensity. The number of ROS events are also recorded for each month of the winter season to identify spatial variations and trends in their seasonality.

3 Results

3.1 Present day climatology and trends in ROS

In Fig. 2 the decadal trend in the mean ROS (a) frequency, (b) duration, (c) total precipitation, and (d) intensity is shown in the upper row for the full CARRA period (1991-2023), while the climatological averages are shown only for the overlapping period of the CARRA (e, f, g, h) and HCLIM-ERA5 (i, j, k, l) datasets (2000-2020) for comparison. Differences between CARRA and HCLIM-ERA5 are illustrated in panels (m), (n), (o) and (p) of Fig. 2. Addressing first the trends since 1991 (grid cells where $p < 0.1$ only), it is evident that significant and increasing trends are found predominantly across eastern and north-eastern areas of the archipelago in all characteristics. For the ROS frequency (Fig. 2(a)), significant and increasing trends are also found in southern and central parts of the archipelago, as well as in the coastal parts of the northeast and across Edgeøya. Across Nordaustlandet, increases of up to 1 event per winter per decade are found around the coastal areas which include both land and glaciated parts. On Spitsbergen, increasing trends of up to 1.5 events per winter per decade are occurring across the central and eastern parts of Nordenskiöld Land as well as the south-eastern parts of Spitsbergen and some coastal areas in the northwest. ROS frequency is also increasing over most of Edgeøya. Examining the trends in the duration, total precipitation, and mean intensity of ROS events, there are also increasing and significant trends, but the geographic variations are somewhat different compared to the trends in ROS frequency. For ROS duration (Fig. 2(b)), significant and increasing trends are mainly confined to low-lying valley areas across Nordenskiöld Land and southern Spitsbergen but on Nordaustlandet increasing trends are exhibited around the entire coast of the island, and in general the decadal trends are also greatest here, with increases of up to 0.5 days per event. Related to the increasing trend in ROS duration is an increasing trend in the total precipitation (Fig. 2(c)) and intensity (Fig. 2(d)), which is exhibited across the same areas on Nordaustlandet. Typical trends in these areas are of the order 2 mm per event per decade for total precipitation and around 1mm/day per decade in ROS intensity. Somewhat larger increases in total precipitation of 4-5mm per event (per decade) are found on Edgeøya and Barentsøya.

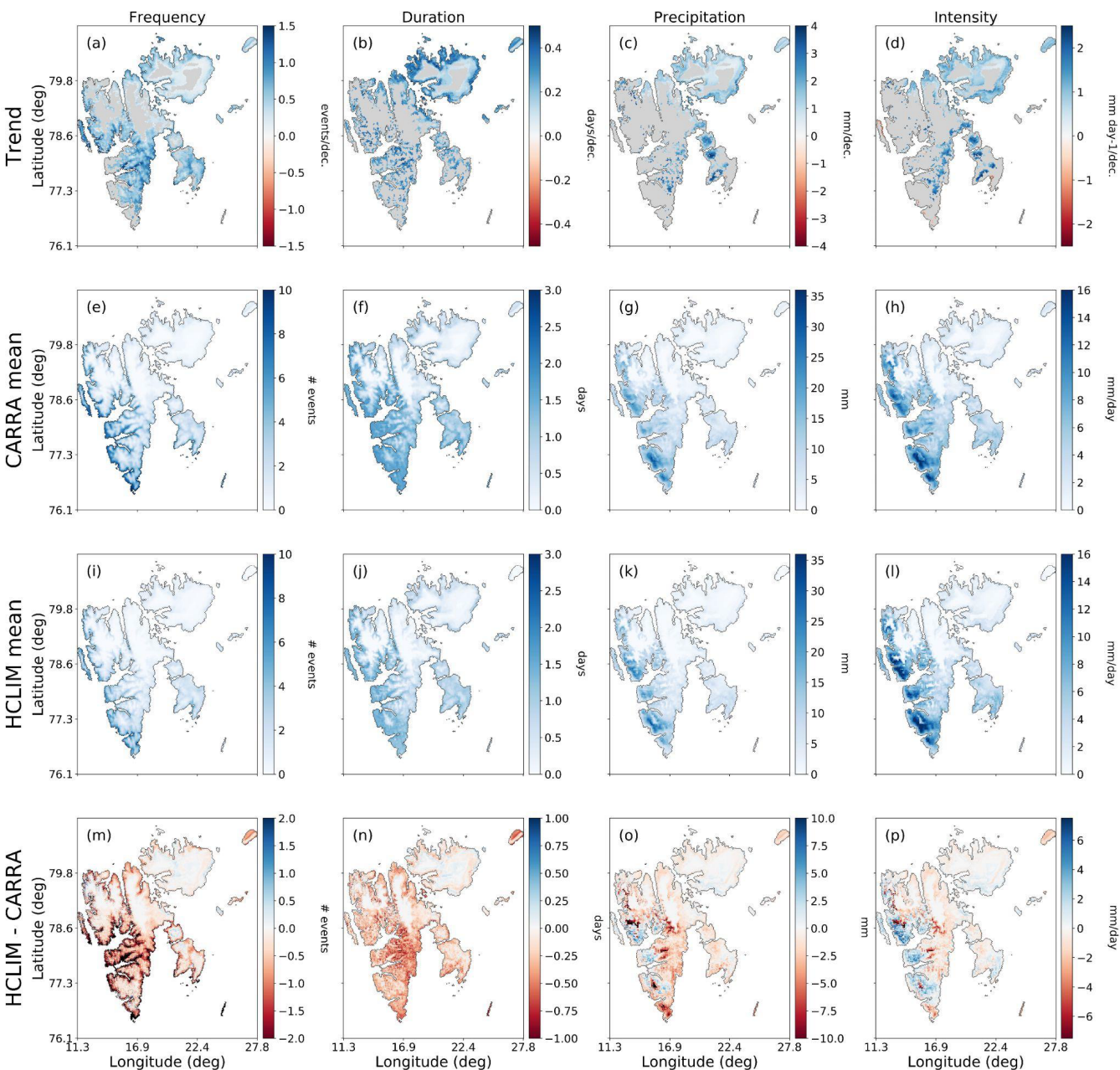


Figure 2: Present day trends (a) to (d) and climatology of ROS frequency, duration, total precipitation per event, and mean intensity for 2000-2020 using the CARRA dataset (e, f, g, h) and HCLIM-ERA5 (i, j, k, l) and the difference (m, n, o, p) between the datasets (HCLIM minus CARRA). Trends in (a) to (d) are obtained for the entire CARRA period (1991-2023).

Comparing the climatological averages of the characteristics obtained using CARRA (Fig. 2 (e) to (h)) and HCLIM-ERA5 (Fig. 2(i) to (l)) for the present climate, the geographical variations are reproduced reasonably well by the HCLIM-ERA5 dataset even though the absolute values for all characteristics are lower with respect to the CARRA output for the ROS



frequency and duration. The difference is typically of the order of 1 event and 1 day respectively, with CARRA showing higher values over most of the archipelago, except for across the larger glaciated areas over Nordaustlandet where HCLIM-ERA5 dataset tends to show slightly more ROS events than the CARRA simulations. For ROS frequency, both CARRA and HCLIM-ERA5 show that there is a southwest-northeast gradient, with ROS occurring most frequently in the southwest and western coastal areas of Spitsbergen and decreasing across inland areas. However, while ROS are at present occurring least frequently across eastern and inland areas of the archipelago, one may note that it is these areas where ROS have been increasing in frequency during the past 30 years (Fig. 2 (a)). The same climatic gradients are exhibited by the averages of ROS duration, total precipitation, and intensity. However, the contrast between western and southwestern coastal areas and inland areas of Spitsbergen is not so prominent for ROS duration as it is for total precipitation and intensity.

The mean duration of ROS events is of the order of 1-2 days across the southern, central, and north-western parts of Spitsbergen, with an overall agreement in both the CARRA and HCLIM-ERA5 datasets. However, comparing the mean ROS total precipitation and intensity, HCLIM-ERA5 tends to estimate higher total precipitation in the western regions compared to CARRA, even though the mean event duration is only marginally lower, leading to an overall higher event intensity in the HCLIM-ERA5 dataset in these western regions. The lower intensity in these regions in the CARRA dataset is likely the result of slightly longer ROS durations estimated by CARRA, while total precipitation is also overall lower than HCLIM-ERA5 in these areas. On the other hand, CARRA tends to estimate higher total precipitation across the more eastern and southern parts of the archipelago, as well as in parts of the north. However, the greatest differences between the datasets for the mean total precipitation are typically only of the order 3 to 4mm per ROS event.

Figure 3 decomposes the trend in ROS frequency by month using the CARRA dataset from 1991-2023. Only significant trends are shown, while non-significant trends are indicated by the grey shading. It is striking to note that ROS frequency has increased significantly in predominantly two months of the winter season; late autumn (November) and mid-winter (February). Moreover, the geographical distribution of the significant trends is different and contrasting for these months; in November, increasing trends in ROS frequency are predominantly found around the coastal areas of Nordaustlandet, eastern Spitsbergen and Edgeøya, areas typically associated with a colder inland climate, while in February the significant and increasing trends are found only along the entire western coast of Spitsbergen and parts of southern Spitsbergen, typically associated with a milder maritime climate. The trends exhibited in ROS frequency exhibited in Fig. 3 thus originate mainly from changes in ROS frequency during November and February, while ROS frequency during all other months of the winter have not changed significantly since 1991.

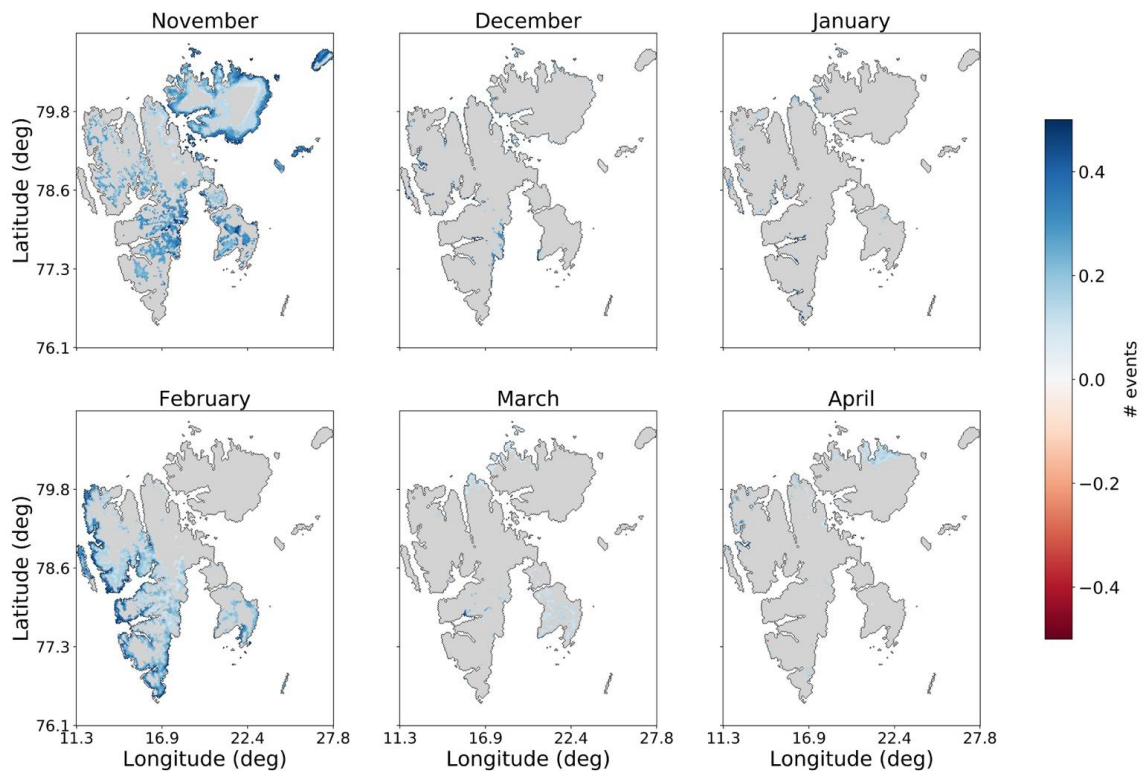


Figure 3: Trend in number of events per month for the 1991-2023 CARRA period

In Sect. 3.2 we have examined the expected changes in ROS during the next four decades under a high emissions scenario, obtained using the climate projections from HCLIM-MPI.

3.2 Projected future changes in ROS characteristics

Figure 4 shows the projected change in the mean number of ROS events, the mean duration, total precipitation, and intensity in the 2030-2050 and 2050-2070 periods, compared to the mean for the historical period (2000-2020). In terms of the absolute changes, Fig.4 shows that for both the future periods examined, 2030-2050 and 2050-2070, the frequency of ROS events is projected to increase most over the same areas where significant and increasing trends in frequency were identified in Fig.2. That is to say, the areas that exhibit the greatest increase in number of ROS events are across the eastern, southern, and northern parts of Spitsbergen, as well as across Edgeøya. The change in mean number of events for the 2050-2070 period could be twice as great as for the 2030-2050 period, as indicated by the different colour scales used in Fig.4. The geographical variation in change in ROS events is somewhat different to the geographical variations in ROS frequency for the present climate and does not exhibit similarities to the geographical variations in significant trends since 1991 (Fig. 2). Figure 4 shows that the mean duration of ROS events may increase by up to 1 day by 2030-2050, with the largest increases in duration occurring in the northern and north-eastern parts of the archipelago, as well as weaker increases in mean ROS duration across eastern parts



of Nordenskiöld Land and Edgeøya. Thus, ROS duration is projected to increase most over glaciated and mountainous areas in the northern part of the archipelago, where there are very few, if any, ROS events in the present climate (Fig. 2). This is likely due to an overall increase in wintertime temperatures, leading to a greater probability of days above freezing with precipitation than in the present climate. However, these areas with the greatest increase in mean ROS event duration currently have a mean duration between 0 to 0.5 days in the present climate, indicating that there are at present only isolated ROS events that do not occur every winter. The mean increase in ROS event duration is typically only of the order of 1 day by the 2050-2070 period over these areas, while the mean increase in number of events in the areas exhibiting greatest increase in duration is of the order of 2-3 events for the same period, indicating that the ROS events that do occur could be typically single-day events. At the same time there are projected decreases in the mean duration, total precipitation and mean intensity of events across the western coastal parts of Spitsbergen by 2030-2050. For the changes in ROS total precipitation and intensity, several specific regions stand out; these are the same areas that are expected to experience greatest increases in ROS duration; the glaciated inland regions in the northwest and some areas close to the east coast of Spitsbergen (≥ 15 mm per event) and across the coastal areas on Nordaustlandet. Notably, the change in total precipitation and intensity by 2050-2070 (with respect to 2000-2020) is only slightly greater than the changes in 2030-2050. This differs from the ROS frequency and duration, where there are projected to be greater increases over large areas in the 2050-2070 period compared to 2030-2050.

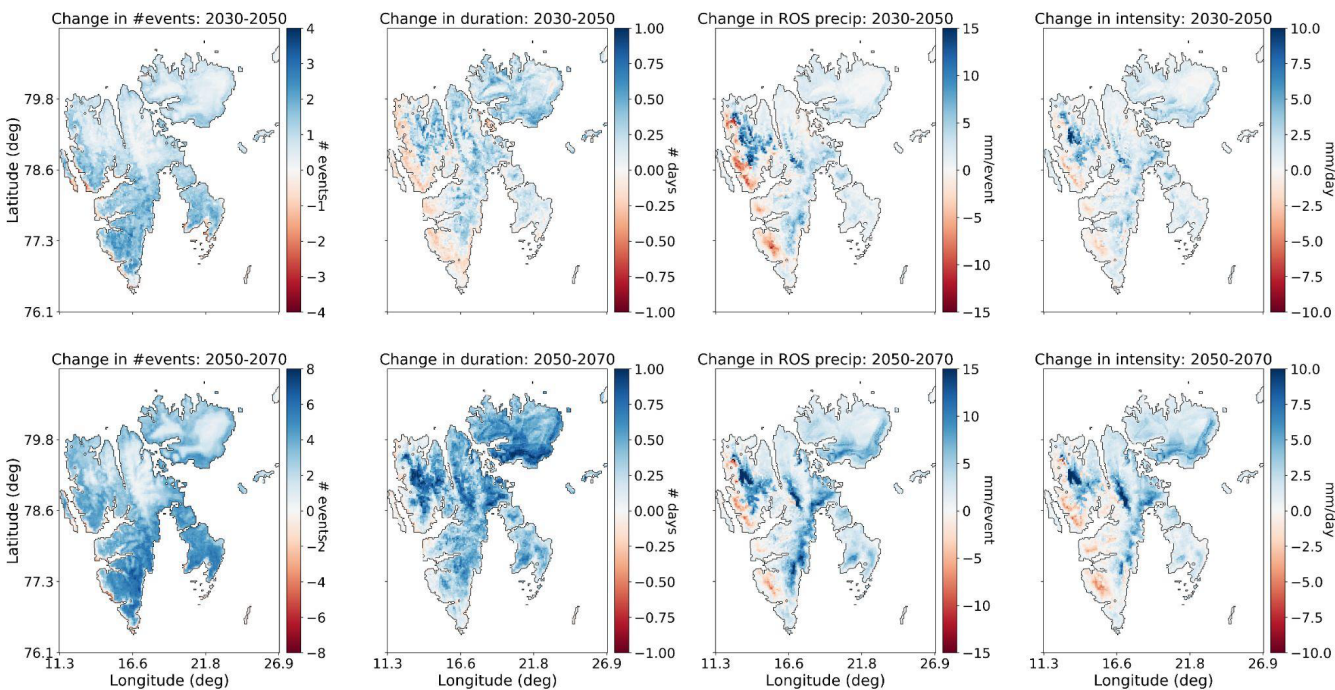


Figure 4: Change in ROS frequency, duration, total precipitation, and mean intensity for 2030-2050 (upper row) and 2050-2070 (lower row) relative to the 2000-2020 averages

Figure 5 also shows the projected changes in the four ROS characteristics but rather expressed as the percentage change relative to the 2000-2020 mean as opposed to the absolute values. This approach illustrates the areas that could experience the most



dramatic changes in the ROS characteristics with respect to the present-day climatology. The glaciated and mountainous regions in northern Spitsbergen and especially across Nordaustlandet are expected to undergo the greatest change relative to the 2000-2020 average. While the percentage changes are very large ($>300\%$ in 2030-2050, $>800\%$ in 2050-2070), it should be recalled that the mean frequency, duration, total precipitation and intensity of ROS events across these areas are at present very low; thus, even a change producing on average one single-day ROS event per winter results in change of several hundred percent relative to the present-day values. Nevertheless, such considerable relative changes over glaciated areas may have considerable impacts on hydrology, which could subsequently have consequences for fjord and marine ecosystems due to freshwater runoff during the wintertime. This will be further discussed in Sect. 4.

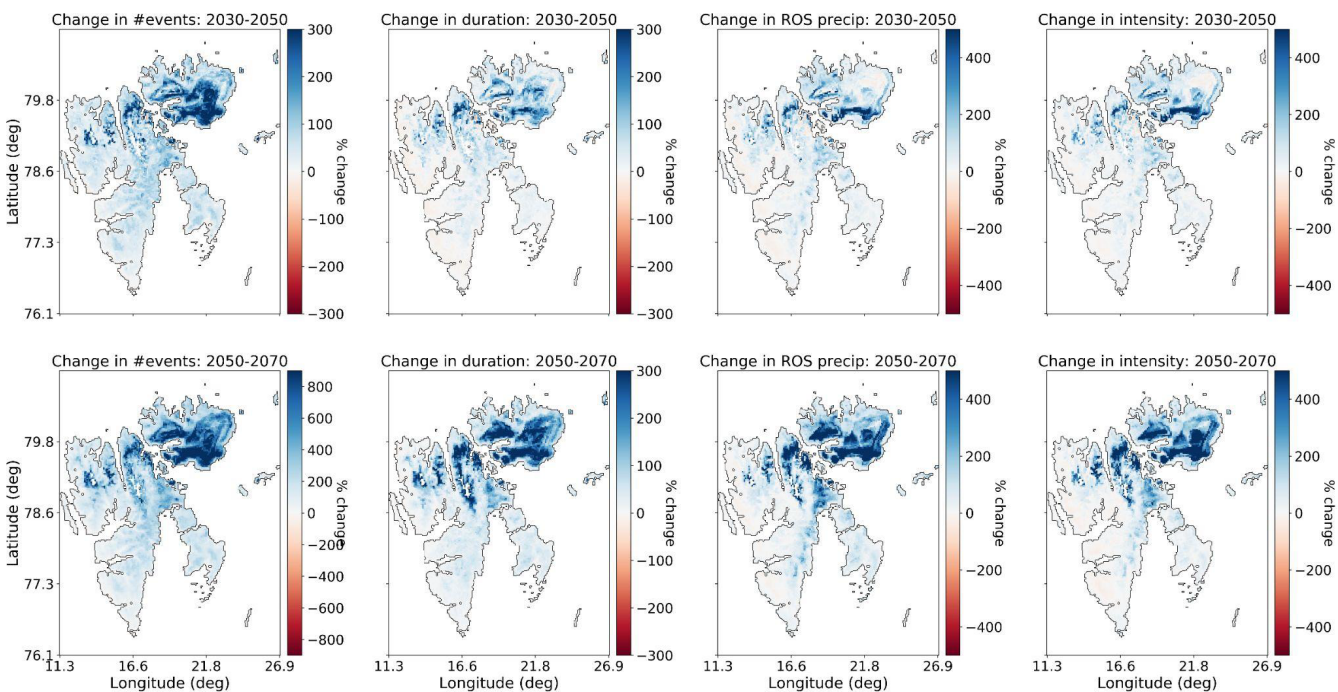


Figure 5: Change in ROS frequency, duration, total precipitation, and mean intensity for 2030-2050 (upper row) and 2050-2070 (lower row) expressed as a percentage of the 2000-2020 averages

In Fig.6 the changes of ROS frequency as shown for each month of the winter period (November-April). For the earlier 2030-2050 period, the greatest increase in the number of ROS events is projected to occur in November across eastern parts of Spitsbergen, as well as across southern parts of Nordaustlandet and on Edgeøya. Decreases in the mean number of events in November are expected along the entire western coast of Spitsbergen. Smaller increases (0.5-1 events) in the mean ROS frequency are projected to take place in January and February, but confined to the north-western, central, and southern parts of Spitsbergen. By 2050-2070 the situation changes quite dramatically. While increases in the mean ROS frequency continue to occur in November and across the same areas during the 2030-2050 period, the greatest changes in ROS frequency (>1.5 events) are projected to occur in April, and these changes are present across large parts of the entire archipelago. Only some glaciated parts of northern Spitsbergen and Nordaustlandet may not experience such great increases in ROS frequency during



April in the 2050-2070 period. Furthermore, changes in ROS frequency of comparable magnitude could also take place during January, a month that has until now not experienced significant changes in ROS frequency (Fig. 2). In Fig.6 it can also be seen that there may be weak decreases in the mean number of ROS events in some areas of the northern and eastern Spitsbergen in December, and across western and southern areas during March for the 2030-2050 period. However, in the later future period (2050-2070) these same areas exhibit increases with respect to 2000-2020.

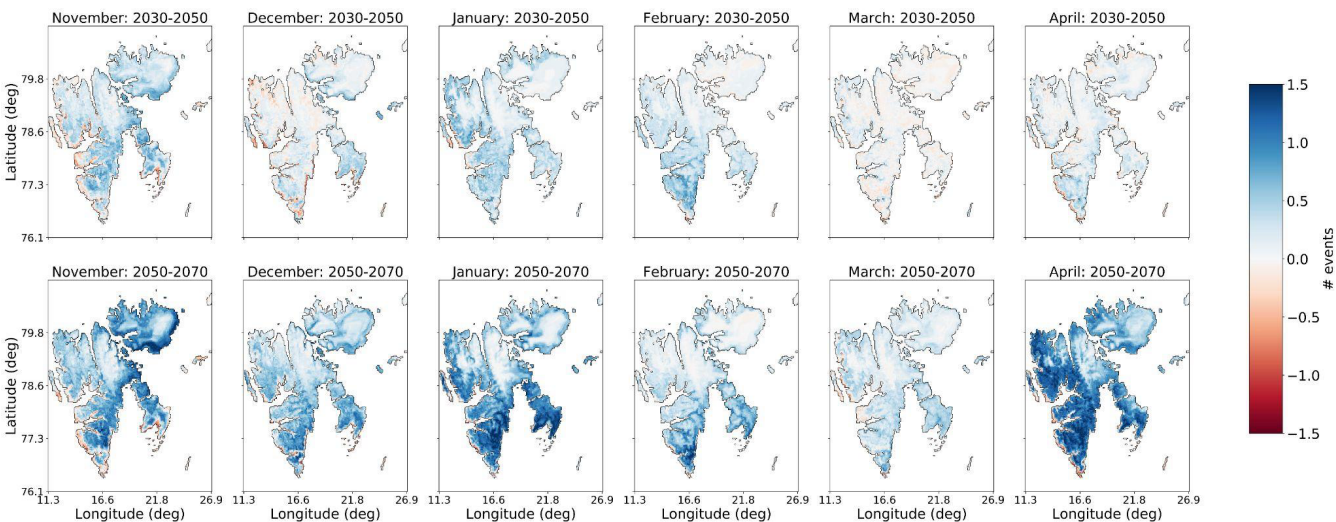


Figure 6: Changes in ROS frequency by month for 2030-2050 (upper row) and 2050-2070 relative to the reference period 2000-2020.

Figure 7 shows the spatial distribution of the absolute change in ROS frequency, duration, total precipitation and intensity for land and glaciers. For the ROS frequency in the near-future period (2030-2050), both land and glacier areas exhibit a change ranging from -1 to +3 events per winter on average compared to 2000-2020, while for the latter period (2050-2070) this change is clearly almost doubled with a range from -2 to +7 events. For glaciers there are no areas experiencing a reduction in frequency for the two periods, while there are some areas with a decrease in frequency across land areas. There is also a clear positive shift in the distribution of change in ROS duration for glaciers compared to the change in mean ROS duration for land areas, which is most prominent for the later future period 2050-2070. While the peaks of the mean duration distributions lie at roughly +0.05 and +0.20 days for land and glaciers respectively in 2030-2050, the peaks lie at +0.3 and +0.5 days for land and glaciers respectively in the 2050-2070 period, indicating a greater increase in ROS duration over glaciers compared to land in this period compared to the earlier 2030-2050 period. Likewise, there is a pronounced shift in the peak of the distribution for ROS intensity over glaciers. While most glacier areas are projected to experience roughly a +1mm/day change in intensity for the 2030-2050 period, for the 2050-2070 many glacier areas exhibit a change in intensity of around +2.5mm/day relative to the 2000-2020 period. For land areas, the overall change in intensity is projected to be +1mm/day for both future periods. For total precipitation, the changes for land and glaciers are mostly positive, and the distributions overlap for both future periods.

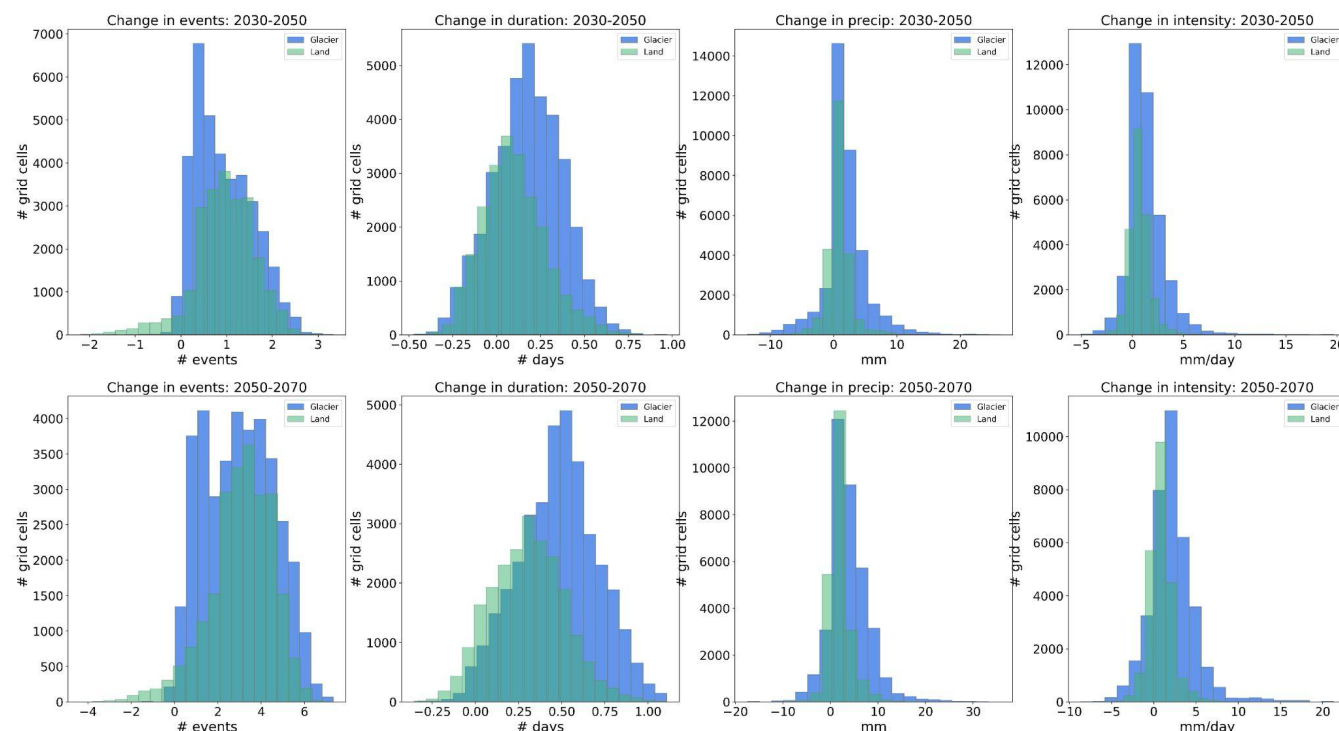


Figure 7: Spatial distribution of change in ROS frequency, duration, total precipitation and mean intensity for 2030-2050 (upper row) and 2050-2070 (lower row) shown for land and glaciers separately.

4 Discussion

This study has utilized a 32-year time series of an atmospheric reanalysis and a 70-year time series of a km-scale climate simulation for Svalbard to (i) study how four characteristics of ROS events have changed in the most recent three decades from 1991 to 2022, and (ii) how they may change in the forthcoming decades, specifically, 2030-2050 and 2050-2070, as represented by one km-scale regional climate model simulation under a high greenhouse gas emissions scenario. Statistically significant increasing trends in all parameters were found predominantly in the lower-lying outskirts of Nordaustlandet in the north-east of the archipelago, and across Edgeøya in the southeast, while significant increases in frequency were also found across the eastern areas of Spitsbergen. No significant trends were found in the western parts of Nordenskiöld Land and southwest Spitsbergen, where ROS frequency is at present greatest. That is to say, the greatest and significant increases in ROS frequency, duration, total precipitation and intensity are found in areas where there are at present very few, if any, ROS during the winter months.

Increasing trends were exhibited by all ROS characteristics since 1991 using the CARRA dataset, but significant trends are confined to Nordaustlandet and Edgeøya, areas that are in closest proximity to sea ice presence during the winter. Sea ice extent around Svalbard has been declining (e.g., Onarheim et al., 2014) and it has been shown to be a key driver of strong warming trends across Spitsbergen (Isaksen et al., 2016, Isaksen et al., 2022) in recent decades. However, whether trends in



sea ice extent may explain where there have been most significant increases in ROS characteristics is nevertheless an open question. Wickström et al. (2020) found that local and regional sea ice extent drives seasonal variations in temperature and precipitation patterns across Svalbard but find less sensitivity of ROS to sea ice presence, as they found that ROS are primarily driven by the advection of warmer air masses from the southerly sector. Other studies of ROS events across the Yamal and Alaska have, on the other hand, noted below average sea ice concentration prior to events, suggesting a link between sea ice concentration and ROS (Forbes et al., 2016; Bartsch et al., 2023). While it has not been the objective of this study to quantify what role sea ice presence plays in the occurrence and characteristics of ROS events, this could be an important topic to consider for future studies, given the rapid and ongoing decline of sea ice around Svalbard and across the polar regions. Comparing the ROS characteristics of the CARRA dataset to those produced for the same period using the regional climate model driven with ERA5, it was found that the regional climate model projections provided by the HCLIM-ERA5 dataset reproduces the overall geographical variations in ROS frequency, duration, total precipitation, and intensity for the present/historical climate qualitatively well. However, the HCLIM-ERA5 dataset estimates slightly lower ROS frequency and duration compared to CARRA dataset over most of the archipelago. More conflicting results were found for the total precipitation and intensity, where HCLIM-ERA5 tended to estimate somewhat higher total precipitation across western areas, where ROS frequency was greatest, but higher total precipitation across eastern and southern parts of the archipelago, where ROS is typically less frequent in the present climate. Overall, the comparison of ROS climatology for the historical period demonstrates that the future projections of ROS characteristics should produce reliable climatologies. The discrepancy in absolute values of the characteristics for the present climate (2000-2020) are likely attributable to the uncertainty in temperature threshold for partitioning rain and snow used in the different datasets. The temperature threshold for the CARRA dataset was determined via calibration against ground observations, and different datasets have been shown to require different temperature thresholds for detecting ROS (Vickers et al., 2024) whereas a calibration has not been done for the HCLIM-ERA5 simulations; therefore, applying the CARRA threshold to the HCLIM-ERA5 dataset cannot be expected to reproduce identical results. Our analyses based on CARRA indicate that there were only significant and increasing trends in ROS frequency since 1991 during November and February, and that the geographical variations in these trends are not the same in both months. While for the early winter ROS in November the greatest trends have occurred over Nordaustlandet and eastern areas of Spitsbergen, in mid-winter (February) the trends in ROS frequency have been strongest across western and southern parts of Spitsbergen. However, in the two future periods examined in the HCLIM-MPI simulation, similar areas will continue to experience an increase in ROS frequency in November, but a decrease is projected along the western and southern coast of Spitsbergen. In contrast these areas will continue to experience an increase in ROS in February. The observed decreases in ROS frequency, duration and precipitation across western areas close to the coast could be attributed to a later onset of the snow season and thus a shorter period for rain to fall on snow. In the present climate there are almost no ROS events anywhere across the archipelago during March and April (Vickers et al., 2024) but the HCLIM-MPI climate projections indicate that, by 2050-2070 April will be the month experiencing the greatest increase in mean number of ROS events. In terms of potential for ground ice formation, April is at present the month with typically greatest snow depths, and ROS events occurring during April



may not contribute significantly to formation of ground ice as thicker snowpacks will typically absorb rain before it reaches the snow-ground interface (Peeters et al., 2019). Moreover, if the onset of spring snowmelt also occurs earlier in the future, then many of the April ROS events may correspond to rain falling on an already isothermal snowpack, which would unlikely result in ground ice but rather increased surface runoff, with knock-on implications for fjord and marine ecosystems. However, since there will be similar increases in ROS events across large parts of the archipelago during late autumn/early winter, the November ROS events may result in early formation of ground ice, thereby creating the potentially difficult foraging conditions for herbivores such as reindeer that persists throughout the winter. On the other hand, a later onset of snow and thinner early winter snowpack, coupled with more frequent and intense ROS could lead to complete ablation of the snow cover, providing greater access to forage. The future situation of ground ice formation due to ROS and its associated impacts on ecosystems is therefore challenging to foresee based on atmospheric parameters alone.

Our analysis of the HCLIM-MPI climate projections show that large areas of the archipelago are projected to undergo an increase in ROS frequency and duration by 2030-2050 and 2050-2070. Areas in the south and east of Spitsbergen are projected to experience the greatest increase in ROS frequency, but it is primarily the glaciated regions in the north and northeast that exhibit the greatest changes relative to the frequency in the present climate, while decreases in several of the ROS characteristics may occur along the western and southwestern coast. The parts of the archipelago exhibiting greatest relative change in ROS characteristics have earlier been shown to be the same areas with greatest projected decrease in average winter snow depths (Isaksen et al., 2017), primarily the glaciated high lying areas north and northeast of Svalbard. Sobota et al. (2020) studied the impact of ROS events over small glaciers in northwestern Spitsbergen and found an increase over the period 1976-2018 resulting in more ice layers, noting that ROS intensity in particular controlled ice layer thickness. Other studies of ROS impacts over glaciers have used snow model simulations or in-situ observations and shown that ROS events may increase the wintertime glacier mass balance as percolated water refreezes in the snowpack (eg., van Pelt et al., 2016; Łupikasza et al., 2019), while a recent review of winter warm spells and heat waves highlights potential alteration of the glacier thermal regime when snow falls at relatively warm temperatures (Spolaor et al., 2025). Indeed, a recent study combined a set of ice core observations together with modelling of glacier stratigraphy and identified a transition in the thermal regime and stratigraphy of Austfonna in the northeast of Svalbard since 2013, from cold to temperate firn above the ice-firn interface (Innanen et al., 2025). In areas with large snow accumulation, multiple ROS events throughout the winter will contribute to ice layers forming within the snowpack, which will influence how rainwater from subsequent ROS events percolates through the snowpack, with knock-on impacts for runoff generation. Overall, it is clear that the snowpack characteristics may be impacted by the significant increases in ROS that are expected to take place over Svalbard's glaciers within the next 50 years. While these areas may not be significant for land-based herbivores, increased melt and/or runoff from glaciers could have indirect ecological impacts by contributing with freshwater input to coastal or fjord environments, with subsequent impacts on fjord biogeochemistry and ecosystems (e.g. Vonnahme et al., 2023).



Limitations of the study

This study has utilized a regional climate model to downscale a global climate model. While this allows for an improved simulation of precipitation over smaller spatial scales which is crucial for mountainous and glaciated areas such as Svalbard, the use of only one RCM and one GCM is a major limitation in capturing model parameterisation uncertainty and internal climate variability. Moreover, there remains a large degree of uncertainty in the magnitude and patterns of precipitation changes simulated by GCMs at local scales, limiting their use in risk assessments. Future work could for example use an ensemble of models to produce a more robust projection of changes in ROS characteristics to identify similarities or discrepancies in the patterns of change across different models.

Our approach utilizes daily values of meteorological (mean air temperature, precipitation) and surface (snow depth water equivalent) variables to detect days with rain-on-snow. These variables are commonly available across different reanalysis and climate model datasets which therefore makes the approach reproducible for other regions of the world where the impacts of ROS are consequential. However, a weakness in this approach is that the rain-snow transition is not properly represented. RCMs at km-scales offer a physics-based approach as the precipitation processes are represented exclusively by the microphysical scheme which separates precipitation into liquid and solid forms based on physics. This contrasts with coarser RCMs which must use both a microphysics scheme and a cumulus scheme, the latter of which cannot separate precipitation into liquid and solid form explicitly, thus necessitating the use of temperature-based approach. We have attempted to address this aspect by comparing the climatologies of each ROS characteristic for the 2000-2020 period using the HCLIM-ERA5 dataset, using temperature thresholds ranging from -0.5°C to 0.5°C , and when using the *prrain* variable, which gives 3-hourly estimates of the precipitation falling as rain (Figure A1). While there was better agreement between the *prrain*-based detection of ROS, and the temperature-thresholded approach using $T=-0.5^{\circ}\text{C}$ for the ROS frequency and duration for the archipelago as a whole, this temperature threshold produced much greater estimates of ROS total precipitation and intensity, especially in the western and southern parts of the archipelago. This is most likely an effect of taking a daily precipitation sum on days where the daily mean temperature exceeded this threshold. Whereas the *prrain*-based detection gives the total sum of rain on days with snow cover, the temperature threshold-based approach would most likely overestimate the total precipitation falling as rain, especially if there are wide variations in the daily temperatures. However, it should be highlighted that the temperature-based approach for partitioning rain and snow is nevertheless valid and necessary in cases where datasets have much coarser spatial resolution (eg >12 km) or temporal resolution and still remains the only approach using ground observations where precipitation phase data are unavailable.

Hydrological modelling should also be considered, given that our analysis suggests a shift towards a large increase in ROS frequency in April. While April is a present typically a month with greatest snow depths and sea ice concentration around Svalbard, in a future climate April may be important for the onset of spring snowmelt, thus a large increase in ROS could also increase the potential for flooding impacts through enhanced runoff due to the combination of rain and rain-amplified snowmelt. There is also an uncertainty in how runoff may be affected by the presence of multiple ice layers within a snowpack



caused by increased ROS frequency in areas with large snow accumulations. These impacts could be addressed in greater detail to follow up the initial results presented here. Moreover, the potential link between sea ice concentration and ROS events should be more carefully assessed and quantified, given the impact of continued rapid climate warming in the polar regions on sea ice cover.

5 Conclusion

This study has examined five specific characteristics of rain-on-snow events across Svalbard in the present climate using the CARRA reanalysis dataset, and in the future climate using a km-scale simulation from HCLIM. ROS frequency, duration, total precipitation, intensity and seasonality were quantified. We found significant and increasing trends in all characteristics, but the significant trends were confined mainly to areas around the low-lying parts of Nordaustlandet and some areas in the east of the archipelago, while southern and western areas that typically exhibit greatest values in all characteristics, were not found to exhibit significant trends since 1991. Using the same approach to quantify ROS, the HCLIM dataset driven by ERA5 input showed good agreement in the geographic variability of all characteristics, though there were small differences in the absolute values. The downscaled global climate projection from 2030 to 2070 revealed that the greatest changes relative to present day conditions in all ROS characteristics are expected in the mountainous and glaciated areas in the north and northeast of the archipelago, while low lying western coastal areas will experience a decrease in all characteristics, most likely attributable to the result of fewer days with snow. Lastly, our analysis indicates that ROS have been increasing most in November and February, but in contrasting areas of the archipelago. While ROS have increased most in the eastern and northeastern parts of Svalbard in November, areas that are typically sensitive to sea ice concentration, it is primarily the western and southern parts of Spitsbergen that have experienced significant increases in ROS frequency in February. The projections of Svalbard's future climate features an increase in ROS events across all months, but most substantially in April for the 2050-2070 period, a month which currently experiences very few, if any, ROS events. This shift in ROS timing may have a cascade of impacts for both terrestrial and marine ecosystems that are dependent on snow and snowmelt.

Data Availability

The CARRA dataset is publicly available and can be downloaded from the Copernicus Climate Data Store (CDS). The HCLIM regional climate simulations used in the analysis are available from <https://thredds.met.no/thredds/catalog/pcch-arctic/catalog.html>



Author Contribution

HV and PM designed the study, OL prepared and made available the climate simulations, HV carried out the data analysis and prepared the manuscript with contributions from all co-authors.

Acknowledgements

This research was funded by Svalbard's Environmental Protection fund (grant 24/20) and the Framsenter research cooperation (incentive project CHORUS), and the Norwegian Research Council, project "PCCH-Arctic", under grant ID 320769. The climate simulations were carried out on the Norwegian Research Infrastructure Services (NRIS) high-performance computing facility "Betzy", operated by Sigma2, under project number NN9875K.

We acknowledge the support of PolarRES (grant no. 101003590), a project of the European Union's Horizon 2020 research and innovation programme. Storage and computing resources necessary to conduct the analysis were provided by Sigma2 – the national infrastructure for high-performance computing and data storage in Norway (project nos. NS8002K and NN8002K).

References

Bartsch, A., Bergstedt, H., Pointner, G., Muri, X., Rautiainen, K., Leppänen, L., Joly, K., Sokolov, A., Orekhov, P., Ehrich, D., and Soininen, E. M.: Towards long-term records of rain-on-snow events across the Arctic from satellite data, *The Cryosphere*, 17, 889–915, <https://doi.org/10.5194/tc-17-889-2023>, 2023.

Belušić, D., de Vries, H., Dobler, A., Landgren, O., Lind, P., Lindstedt, D., Pedersen, R. A., Sánchez-Perrino, J. C., Toivonen, E., van Uft, B., Wang, F., Andrae, U., Batrak, Y., Kjellström, E., Lenderink, G., Nikulin, G., Pietikäinen, J.-P., Rodríguez-Camino, E., Samuelsson, P., van Meijgaard, E., and Wu, M.: HCLIM38: a flexible regional climate model applicable for different climate zones from coarse to convection-permitting scales, *Geosci. Model Dev.*, 13, 1311–1333, <https://doi.org/10.5194/gmd-13-1311-2020>, 2020.

Day, J. J., Bamber, J. L., Valdes, P. J., and Kohler, J.: The impact of a seasonally ice free Arctic Ocean on the temperature, precipitation and surface mass balance of Svalbard, *The Cryosphere*, 6, 35–50, <https://doi.org/10.5194/tc-6-35-2012>, 2012.

Forbes, B. C., Kumpula, T., Meschtyb, N., Laptander, R., Macias-Fauria, M., Zetterberg, P., Verdonen, M., Skarin, A., Kim, K. Y., Boisvert, L. N., Stroeve, J. C., & Bartsch, A.: Sea ice, rain-on-snow and tundra reindeer nomadism in Arctic Russia, *Biology Letters*, 12(11), 20160466. <https://doi.org/10.1098/rsbl.2016.0466>, 2016.



- 450 Førland E. J., Benestad, R.E., Hanssen-Bauer, I., Haugen, J.E. and Skaugen, T.E.: Temperature and Precipitation Development
451 at Svalbard 1900–2100, *Adv. Meteor.*, 2011, 1–14, doi:10.1155/2011/893790, 2011.
- 452
- 453 Gutjahr, O., Putrasahan, D., Lohmann, K., Jungclaus, J. H., von Storch, J.-S., Brüggemann, N., Haak, H., and Stössel, A.: Max
454 Planck Institute Earth System Model (MPI-ESM1.2) for the High-Resolution Model Intercomparison Project (HighResMIP),
455 *Geosci. Model Dev.*, 12, 3241–3281, <https://doi.org/10.5194/gmd-12-3241-2019>, 2019.
- 456
- 457 Hansen, B. B., Isaksen, K., Benestad, R. E., Kohler, J., Pedersen, Å. Ø., Loe, L. E., Coulson, S. J., Larsen, J. O., & Varpe, Ø.:
458 Warmer and wetter winters: Characteristics and implications of an extreme weather event in the High Arctic. *Environmental*
459 *Research Letters*, 9(11), 114021, <https://doi.org/10.1088/1748-9326/9/11/114021>, 2014.
- 460
- 461 Hanssen-Bauer, I., Førland, E.J., Hisdal, H., Mayer, S., Sandø, A.B. and Sorteberg, A.: Climate in Svalbard 2100. NCCS Rep.
462 1/2019, 205 pp., <https://www.miljodirektoratet.no/globalassets/publikasjoner/M1242/M1242.pdf>, 2019
- 463 Hopwood et al., 2020 Hopwood, M. J., Carroll, D., Dunse, T., Hodson, A., Holding, J. M., Iriarte, J. L., Ribeiro, S., Achterberg,
464 E. P., Cantoni, C., Carlson, D. F., Chierici, M., Clarke, J. S., Cozzi, S., Fransson, A., Juul-Pedersen, T., Winding, M. H. S.,
465 and Meire, L.: Review article: How does glacier discharge affect marine biogeochemistry and primary production in the
466 Arctic?, *The Cryosphere*, 14, 1347–1383, <https://doi.org/10.5194/tc-14-1347-2020>, 2020.
- 467
- 468 Hersbach, H., Bell, B., Berrisford, P., Hirahara, S., Horányi, A., Muñoz-Sabater, J., Nicolas, J., Peubey, C., Radu, R., Schepers,
469 D., Simmons, A., Soci, C., Abdalla, S., Abellan, X., Balsamo, G., Bechtold, P., Biavati, G., Bidlot, J., Bonavita, M., De Chiara,
470 G., Dahlgren, P., Dee, D., Diamantakis, M., Dragani, R., Flemming, J., Forbes, R., Fuentes, M., Geer, A., Haimberger, L.,
471 Healy, S., Hogan, R. J., Hólm, E., Janisková, M., Keeley, S., Laloyaux, P., Lopez, P., Lupu, C., Radnoti, G., de Rosnay, P.,
472 Rozum, I., Vamborg, F., Villaume, S. & Thépaut, J. N.: The ERA5 global reanalysis, *Quarterly Journal of the Royal*
473 *Meteorological Society*, 146(730), 1999–2049. <https://doi.org/10.1002/qj.3803>, 2020
- 474
- 475 Innanen, S., Hock, R., Schmidt, L.S., Schuler, T.V., Covi, F. and Moholdt, G.: Witnessing the transition from cold to temperate
476 firn on Austfonna ice cap, Svalbard through observations and model simulations, *J. Glaciology*, 2025 (under review)
- 477
- 478 Isaksen, K., Nordli, Ø., Førland, E.J., Łupikasza, E., Eastwood, S. and Niedźwiedź, T.: Recent warming on Spitsbergen—
479 Influence of atmospheric circulation and sea ice cover, *J. Geophys. Res. Atmos.*, 121, 11,913–11,931,
480 doi:10.1002/2016JD025606, 2016.
- 481
- 482 Isaksen, K., Førland, E.J., Dobler, A., Benestad, R., Haugen, J.E. and Mezghani, A.: Klimascenarier for Longyearbyen-
483 området, Svalbard, MET Norway Report 14/2017, 2017.



- Isaksen et al., 2022 Exceptional warming over the Barents Sea <https://www.nature.com/articles/s41598-022-13568-5>
- Isaksen, K., Nordli, Ø., Ivanov, B. *et al.*: Exceptional warming over the Barents area. *Sci. Rep.*, 12, 9371, <https://doi.org/10.1038/s41598-022-13568-5>, 2022.
- Køltzow, M., Casati, B., Bazile, E., Haiden, T. and Valkonen, T.: An NWP model intercomparison of surface weather parameters in the European Arctic during the year of polar prediction special observing period Northern Hemisphere 1, *Weather Forecast.* 34, 959–983. doi:10.1175/WAF-D-19-0003, 2019.
- Køltzow, M., Schyberg, H., Støylen, E., and Yang, X.: Value of the Copernicus Arctic Regional Reanalysis (CARRA) in representing near-surface temperature and wind speed in the north-east European Arctic, *Polar Res.* 41, 8002. doi:10.33265/polar.v41.8002, 2022.
- Landgren, O., Lutz, J., Dobler, A., and Isaksen, K.: Multi-decadal convection-permitting climate simulation over Svalbard and its benefit for assessing the future of cultural heritage sites, EMS Annual Meeting 2022, Bonn, Germany, 5–9 Sep 2022, EMS, 2022-556, <https://doi.org/10.5194/ems2022-556>, 2022.
- Landgren, O., Lutz, J., Isaksen, K.: 2.5 km future climate projections for Svalbard under the high emission scenario SSP5-8.5, MET Report 1/2025, ISSN 2387-4201, 2025.
- Łupikasza, E.B., Ignatiuk, D., Grabiec, M., Cielecka-Nowak, K., Laska, M., Jania, J., Luks, B., Uszczyk, A. and Budzik, T.: The Role of Winter Rain in the Glacial System on Svalbard, *Water*, 11(2):334. <https://doi.org/10.3390/w11020334>, 2019.
- Mooney P.A., Sobolowski, S. and Lee, H.: Designing and evaluating regional climate simulations for high latitude land use land cover change studies, *Tellus Dyn. Meteorol. Oceanogr.* 72 1–17, 2020.
- Mooney, P. A., and Li, L.: Near future changes to rain-on-snow events in Norway, *Environ. Res. Lett.* 16, 064039. doi:10.1088/1748-9326/abfdeb, 2021.
- Onarheim, I.H., Smedsrud, L.H., Ingvaldsen, R.B. and Nilsen, F.: Loss of sea ice during winter north of Svalbard, *Tellus A: Dynamic Meteorology and Oceanography*, 66(1), <https://doi.org/10.3402/tellusa.v66.23933>, 2014.



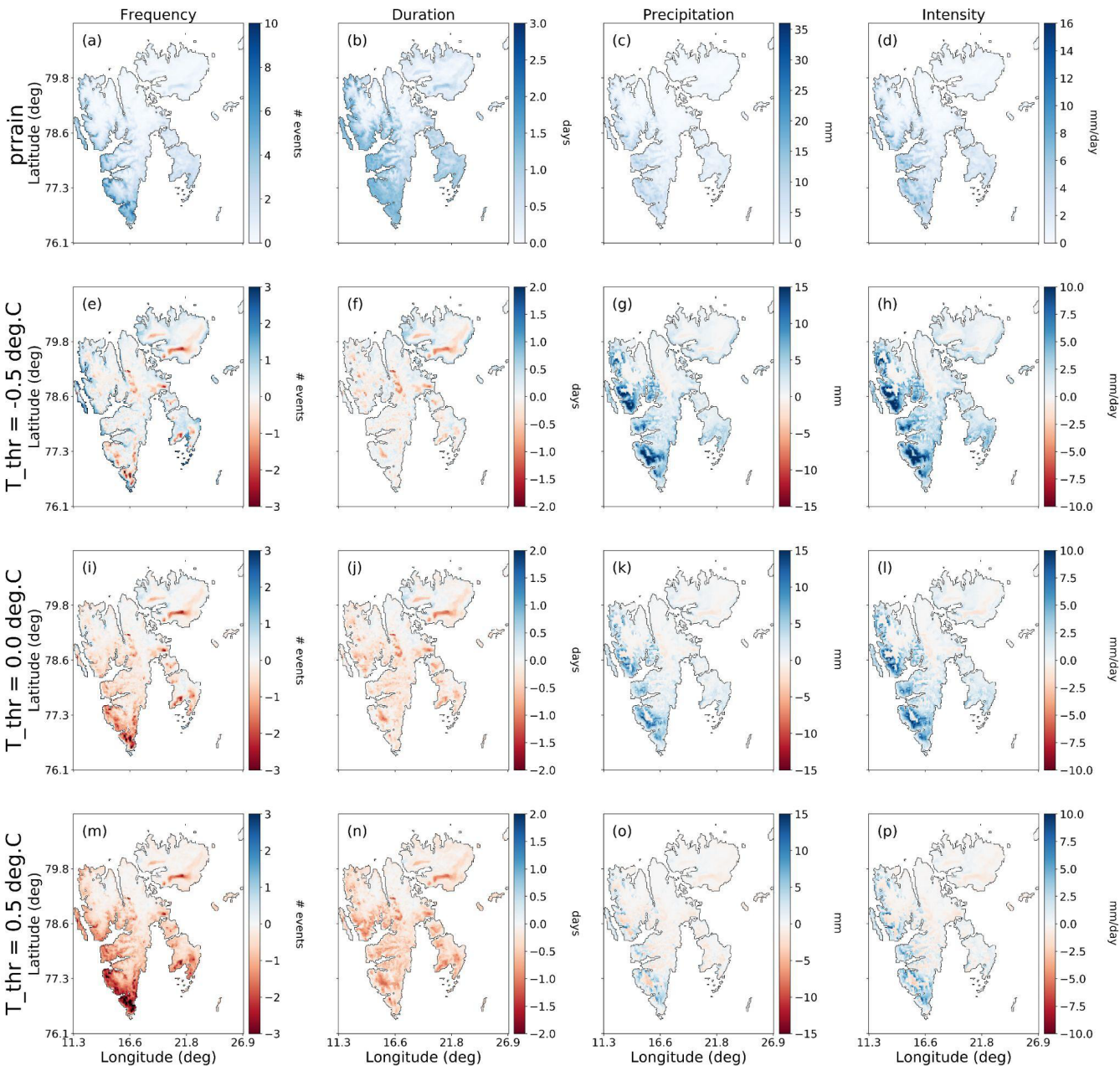
- 516 Pedersen Å.Ø., Beumer, L.T., Aanes, R. and Hansen, B.B.: Sea or summit? Wild reindeer spatial responses to changing high-
517 arctic winters, *Ecosphere*, 12(12):e03883. 101002/ecs2.3883, 2021.
- 518
- 519 Peeters, B., Pedersen, Å. Ø., Loe, L. E., Isaksen, K., Veiberg, V., Stien, A., Kohler, J., Gallet, J. C., Aanes, R., & Hansen, B.
520 B.: Spatiotemporal patterns of rain-on-snow and basal ice in high Arctic Svalbard: Detection of a climate-cryosphere regime
521 shift, *Environmental Research Letters*, 14(1), 015002, <https://doi.org/10.1088/1748-9326/aaefb3>, 2019.
- 522
- 523 Prein, A.F. et al.: A review on regional convection-permitting climate modeling: demonstrations, prospects, and challenges
524 *Rev. Geophys.* 53(2), 323–361, doi: 10.1002/2014RG000475, 2015.
- 525
- 526 Schyberg, H., Yang, X., Køltzow, M. A. Ø., Amstrup, B., Bakketun, Å., Bazile, E., et al.: Arctic regional reanalysis on single
527 levels from 1991 to present, Copernicus Climate Change Service, doi:10.24381/cds.713858f, 2020.
- 528
- 529 Serreze, M., Gustafson, J., Barrett, A.P., Druckenmiller, M.L., Fox, S., Voveris, J., Stroeve, J., Sheffield, B., Forbes, B.C.,
530 Rasmus, S., Laptander, R., Brook, M., Brubaker, M., Temte, J., McCrystall, M.R. and Bartsch, A.: Arctic rain on snow events:
531 bridging observations to understand environmental and livelihood impacts, *Environmental Research Letters*, 16(10), DOI
532 10.1088/1748-9326/ac269b, 2021.
- 533
- 534 Sobota, I., Weckwerth, P. and Grajewski, T.: Rain-On-Snow (ROS) events and their relations to snowpack and ice layer
535 changes on small glaciers in Svalbard, the high Arctic, *Journal of Hydrology*, 590, 125279,
536 <https://doi.org/10.1016/j.jhydrol.2020.125279>, 2020.
- 537
- 538 Spolaor, A., Salzano, R., Scotto, F., Barbaro, E., Luks, B., Laska, M., Sobota, I., Maetze, R., Malnes, E., Vickers, H., Larose,
539 C., Dahlke, S. and Maturilli, M.: Understanding and analysing recurrent warm events in Svalbard: a comprehensive review on
540 land cryosphere (AWARE), SESS report 2024 - The State of Environmental Science in Svalbard - an annual report, 212-226,
541 Svalbard Integrated Arctic Earth Observing System, <https://doi.org/10.5281/zenodo.14425903>, 2025.
- 542
- 543 Van Pelt, W. J. J., Kohler, J., Liston, G.E., Hagen, J.O., Luks, B., Reijmer, C.H. and Pohjola, V.A.: Multidecadal climate and
544 seasonal snow conditions in Svalbard, *J. Geophys. Res. Earth Surf.*, 121, 2100–2117, doi:[10.1002/2016JF003999](https://doi.org/10.1002/2016JF003999), 2016.
- 545
- 546 Vickers, H., Malnes, E., and Eckerstorfer, M.: A Synthetic Aperture Radar Based Method for Long Term Monitoring of
547 Seasonal Snowmelt and Wintertime Rain-On-Snow Events in Svalbard, *Front. Earth Sci.*, 10, 868945,
548 <https://doi.org/10.3389/feart.2022.868945>, 2022.



- 549
- 550 Vickers, H., Saloranta, T., Køltzow, M., van Pelt Ward J. J. and Malnes, E.: An analysis of winter rain-on-snow climatology
- 551 in Svalbard, Front. Earth Sci., 12, <https://doi.org/10.3389/feart.2024.1342731>, 2024.
- 552
- 553 Vonnahme, T.R., Nowak, A., Hopwood, M.J., Meire, L., Sogaard, D.H., Krawczyk, D., Kalhagen, K. and Juul-Pedersen, T.:
- 554 Impact of winter freshwater from tidewater glaciers on fjords in Svalbard and Greenland; A review, Progress in Oceanography,
- 555 219, 103144, <https://doi.org/10.1016/j.poccean.2023.103144>, 2023.
- 556
- 557 Wang, F.: An introduction to the HARMONIE-Climate (HCLIM) regional climate modeling system. Zenodo.
- 558 <https://doi.org/10.5281/zenodo.11424181>, 2024.
- 559
- 560 Wickström, S., Jonassen, M. O., Cassano, J. J., and Vihma, T.: Present temperature, precipitation, and rain-on-snow climate
- 561 in Svalbard. Journal of Geophysical Research: Atmospheres, 125, <https://doi.org/10.1029/2019JD032155>, 2020.
- 562
- 563 Würzer, S., Jonas, T., Wever, N. and Lehning, M.: Influence of initial snowpack properties on runoff formation during rain-
- 564 on-snow events. J. Hydrometeor., 17, 1801-1815, <https://doi.org/10.1175/JHM-D-15-0181>, 2016.



565 **Appendix/Supplementary information**



566
567 **Figure A1. Mean ROS characteristics for the historical period (2000-2020) produced using the HCLIM-ERA5 dataset using the**
568 **accumulated rain variable (prrain) for detection, and the differences between the temperature-thresholded (t_thr) approach using**
569 **thresholds of -0.5°C, 0.0°C and 0.5°C. The difference is given as ROS(t_thr) minus ROS(prrain) such that blue shades indicate areas**
570 **where the temperature-threshold approach produced higher values than prrain, and red areas indicate areas where prrain produced**
571 **higher values of the ROS variable compared to the temperature threshold detection.**

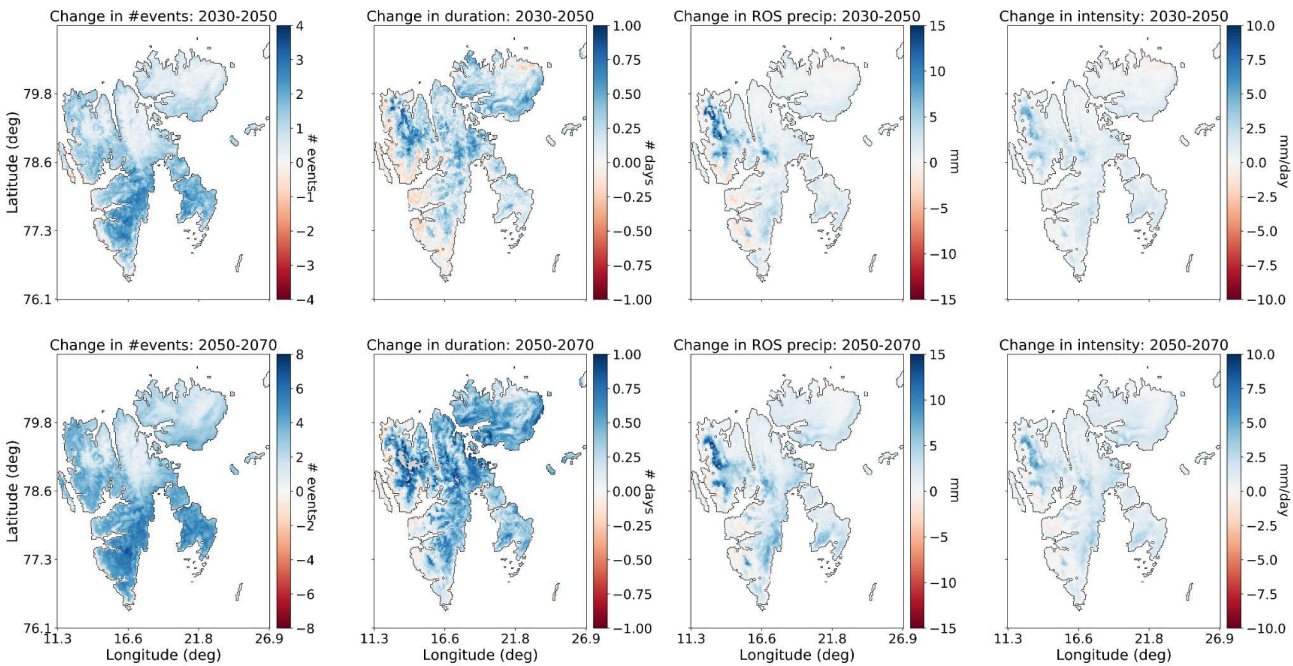


Figure A2. Change in ROS frequency, duration, total precipitation, and mean intensity for 2030-2050 (upper row) and 2050-2070 (lower row) relative to the 2000-2020 averages, using the prrain variable to detect ROS.

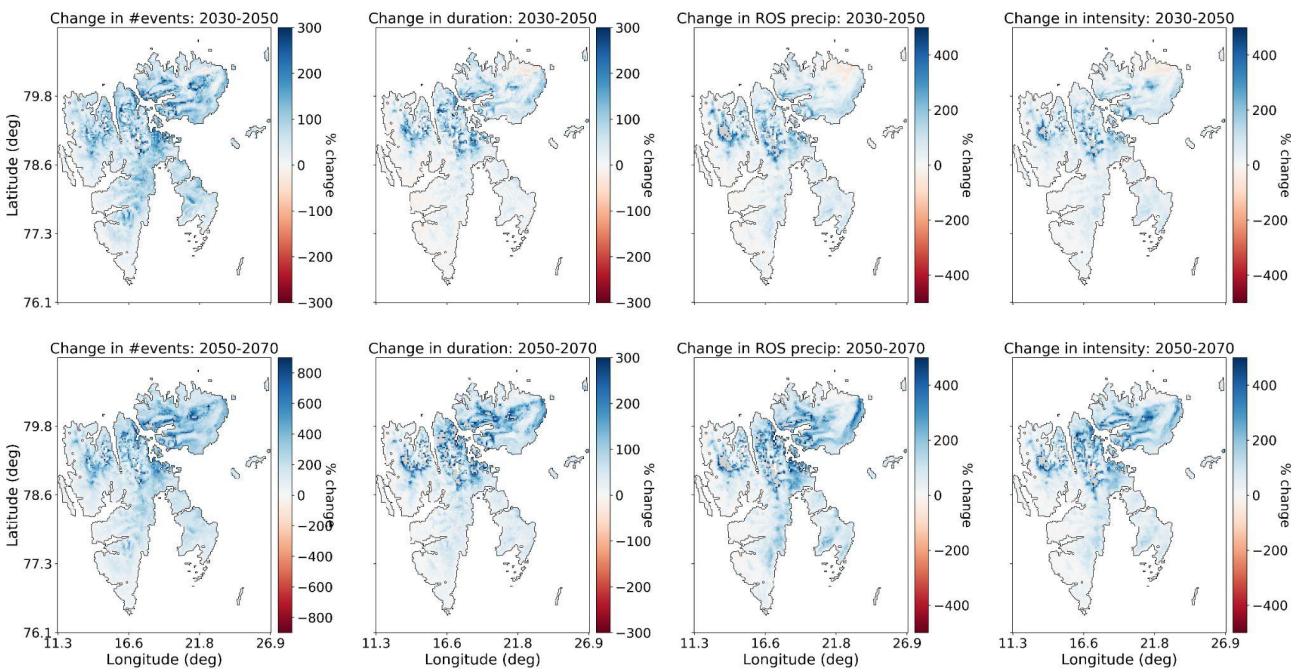


Figure A3. As for Fig. A2 but with the changes expressed as a percentage of the 2000-2020 values.

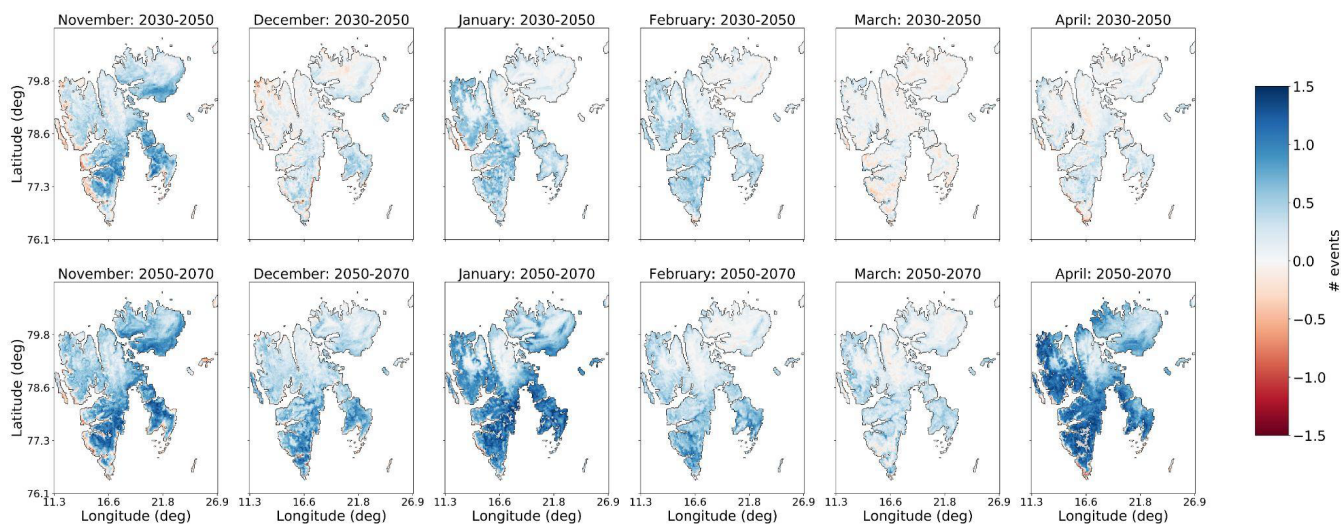


Figure A4. Changes in ROS frequency by month for 2030-2050 (upper row) and 2050-2070 relative to the reference period 2000-2020, when ROS were detected using the prrain variable.